Journal of Emerging Computer Technologies
Research Article
Received: *2023-11-14* | ***Reviewing:*** *2023-11-15 & 2024-02-18* | ***Accepted:*** *2024-02-18* | ***Online:*** *2024-02-18* | ***Issue Date:*** *2023-12-31*
Doi: 10.57020/ject.1390428

Noise Removal from the Image Using Convolutional Neural Networks-Based Denoising Auto Encoder

Younus FAROOQ
Cankiri Karatekin University
Çankırı, Türkiye
younisfarooq321@gmail.com
0009-0006-4512-3989

Serkan SAVAŞ
Kırıkkale University,
Kırıkkale, Türkiye
serkan_savas@hotmail.com
0000-0003-3440-6271

***Abstract*—With the exponential growth in the volume of digital images captured daily, there is an escalating demand for elevating image quality to achieve both accuracy and visual appeal. Addressing this need, the development of techniques for reducing image noise while preserving crucial features, such as edges, corners, and sharp structures, has become imperative. This paper delves into the significance of image denoising and introduces a novel approach utilizing a denoising autoencoder based on convolutional neural networks (CNNs). The proposed method adopts a meticulous two-step process to effectively eliminate noise. Initially, input images are segregated into training and testing sets. Subsequently, a denoising autoencoder model is trained using the designated training data. This model is then further refined through training on a CNN, enhancing its noise reduction capabilities. The evaluation of the system's performance is conducted using testing data to gauge its effectiveness. The study employs the MATLAB programming language for implementation and evaluation. Results, measured through RMSE (Root Mean Square Error) and PSNR (Peak Signal-to-Noise Ratio) criteria on two distinct datasets—the Covid19-radiography-database and SIIM-medical-images—reveal that our proposed method outperforms existing approaches significantly. This approach is particularly promising for applications demanding enhanced image quality, such as the resolution enhancement of medical images. The study contributes to the ongoing efforts in noise reduction research, offering a robust solution for improving visual perception in diverse image processing applications.**

Keywords*—*image noise, denoising autoencoder, convolutional neural network, image denoising.

I. INTRODUCTION

The surge in daily digital image capture has created a rising demand for images that are not only more accurate but also visually appealing. However, this surge in image capture also brings inevitable noise, diminishing overall image quality. Noise significantly impacts image quality in various applications like machine vision and object detection [1], as it can lead to false detections and inaccurate segmentations. Presently, most methods for noise removal primarily target grayscale image noise and struggle to effectively identify all compromised pixels. Various factors contribute to the noise that plagues digital images, including data transmission over noisy channels, hardware storage errors, and defective pixels during image capture [2]. Image denoising's primary objective is to preserve image structures, such as features, edges, and textures. Removing all types of noise before image analysis is crucial to prevent misinterpretation [3], [4]. An image denoising method's effectiveness hinges on how much noise it eliminates and how closely it preserves the original pixel values. Ineffective denoising can result in the loss of vital details, such as edge information. Over the past decades, experts have strived to develop efficient and accurate denoising techniques that reduce noise while maintaining essential visual characteristics [5]. Historically, image denoising methods relied on specific filters designed for certain distributions, rendering them less efficient when distribution characteristics weren't met. Recently, machine learning approaches have gained traction in noise reduction, with neural networks standing out. These algorithms attempt to predict the transformation of input data to output by learning from input-output pairs. Deep learning (DL) algorithms, which aim to mimic human observation, analysis, learning, and decision-making, have seen notable success in complex tasks, especially in diagnostics. DL's popularity stems from advances in on-chip processing, affordable hardware, and research in machine learning and signal processing [5]. DL techniques have particularly gained attention in image noise removal. Autoencoders, a type of neural network, aim to learn an approximation of the identity function using backpropagation [6]. Image denoising is another application of autoencoders, where they serve as non-linear functions to eliminate image noise. Fig. 1 illustrates an overview of an autoencoder.

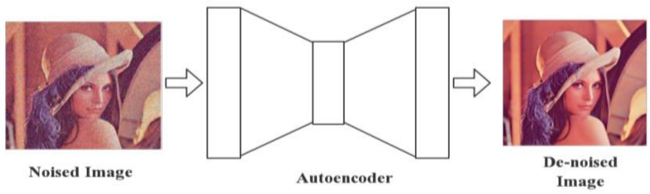

Fig. 1. A view of a denoising autoencoder [7]

In this research, a novel approach employs Denoising Autoencoders (DAE) in conjunction with Convolutional Neural Networks (CNN) to tackle image noise. Autoencoders have become a valuable framework for unsupervised learning of internal representations. This study utilizes a DL-optimized DAE model named CDAE for noise reduction. The CDAE model combines both CNN and DAE, offering a practical solution that works effectively regardless of the noise distribution in images. This network is trained by introducing random noise (specifically Gaussian noise) to the input image, with the objective of producing a noise-free original image as the output. This training strategy encourages the autoencoder to learn a function that removes noise and reconstructs the image. While existing image denoising methods have performed well, they suffer from drawbacks like manual

Cite (APA): Farooq, Y., Savaş, S. (2023). Noise Removal from the Image Using Convolutional Neural Networks-Based Denoising Auto Encoder. *Journal of Emerging Computer Technologies*, 3(1), 21-28. Doi: 10.57020/ject.1390428

parameter adjustments and specific model requirements. Recent advancements in DL, particularly the flexible CDAE architecture, have addressed these issues, making them more practical for real noisy images.

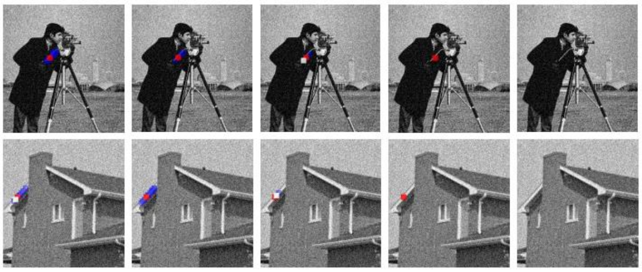

Fig. 2. The matching process of BM3D noise removal

The removal of noise from low-quality images is crucial in many fields, especially in the context of information sharing through digital images. Noise is an inevitable factor in image recognition, significantly degrading visual quality. Hardware issues, software operations like format conversion, copying, scanning, printing, and compression can introduce noise to images. This noise represents an unwanted signal recorded in the image. Consequently, noise removal is a fundamental step in image processing for various computer systems [8], [9]. Image denoising techniques aim to eliminate noise and restore image clarity. Distinguishing between noise, edges, and texture, all of which exhibit high-frequency components, poses a significant challenge in this field. Notably, the types of noise discussed in the literature encompass additive white Gaussian noise (AWGN), impulse noise, quantization noise, Poisson noise, and speckle noise [10]. AWGN originates from analogy circuits, while other noise types result from manufacturing flaws, bit errors, and low photon counts [11]. Image noise removal methods find application in diverse fields such as medical imaging, remote sensing, military surveillance, biometrics, forensics, industrial automation, agriculture, and human identification. In medical and biomedical imaging, denoising algorithms are crucial for eliminating noise types like speckle, Rician, and quantum noise. Remote sensing leverages noise reduction algorithms to address issues like AWGN and salt-and-pepper noise [12]. Military surveillance relies on synthetic aperture radar imagery, where denoising techniques have successfully reduced speckle artifacts. Image denoising techniques originated in the 1960s, initially employing two methods: transformation coefficients such as Fourier transform, discrete cosine transforms, and certain wavelets, as well as pixel value averaging. However, these methods often yielded substantial errors and adverse effects like excessive smoothing, stair-stepping, and ringing, resulting in reduced image quality [12]. In 2005, a novel approach called non-local averaging emerged. Unlike local averaging, which softens images by calculating pixel averages in the vicinity, this method computes the average of all image pixels using patches. Weights are assigned based on similarity to the desired pixel. This approach, exemplified by the block-matching and 3D filtering (BM3D) method, enhances image clarity and retains more details compared to local averaging [13]. Fig. 2 illustrates the process, where a 2D image is treated as 3D. It begins by estimating a noise-reduced image and then iteratively refines noise removal by assessing pixel similarities. Consequently, the image quality heavily relies on pixel similarity, yielding better results when pixels exhibit greater similarity [13].

In this context, the structure of the study is as follows. The second section describes the related studies, and the third section explains the methodology and materials applied. The fourth section describes the results obtained and the fifth section discusses these results. The sixth section concludes the study.

II. Related Works

Efficient learning models were introduced, capable of directly deriving the desired output from input data while conserving energy. Initially, these DL networks processed images in small patches, gradually enhancing results through architectural improvements, advanced cost functions, and newer activation functions. Kamal Bajaj and colleagues introduced a deep learning model based on autoencoders for image denoising, focusing on learning noise from training images to produce clean images [14]. The architecture comprises layers of Convolution, Pooling, Deconvolution, and up sampling, forming a self-encrypting block with a total of 15 layers. Two key objectives guide the establishment of connections between layers: increasing depth to extract more image features and preventing gradient disappearance during network training for improved image reconstruction. Performance evaluation metrics include signal-to-noise ratio and structural similarity index. [15] developed a large-scale denoising convolutional neural network (DnNCC) to remove JPEG compression noise, demonstrating high artifact removal performance with an improved learning algorithm. This technique aids in reducing artifacts, including motion artifacts in diagnostic images. [16] introduced the denoising autoencoder (DAE), demonstrating superior performance compared to traditional examples. [17] devised an adaptive multi-column deep neural network (DNN) with multi-stack sparse DAEs (SSDAE) to handle images corrupted by three types of noise. [18] combined denoising autoencoders (DAEs) and convolutional autoencoders (CAEs) for medical image denoising. [19] introduced a cumulative denoising autoencoder (SCDAE) with a hierarchical structure, embedding whitening layers to process input feature maps. [20] utilized a convolutional denoising autoencoder (CDAE) followed by a DAE in a cascaded fashion to address images with massive noise, highlighting the need for robust image classification systems that perform well across variable noise levels without extensive training.

In the Noise2Noise algorithm [21], the network is trained to perform image denoising solely based on noisy data, without any knowledge of the ground truth. This concept is further extended by the Noise2Void algorithm [22], which eliminates the necessity for pairs of noisy images during training. This feature is particularly pertinent in biomedical applications where ground truth images may be unavailable. A self-supervised approach is introduced by the Noise2Self method [23], obviating the need for prior information on the input image, noise estimation, or ground truth data. Image denoising [24] is accomplished through a convolutional neural network (CNN) extracting features from the noisy image. This method incorporates both edge regularization and total variation regularization. The combination of CNN and low-rank representation is deployed to identify anomalous pixels in hyperspectral images [25]. For restoring blurred images affected by Cauchy noise, a multilevel wavelet convolutional neural network is applied [26]. The Block Matching Convolutional Neural Network (BM-CNN) [27] integrates deep learning with the 3D block-matching method, predicting the denoising of stacks through a DnCNN [28] trained on a dataset comprising 400 images, corresponding to over 250,000 training samples. A feed-forward Convolutional Neural Network is employed for smoothing images independently of the noise level, utilizing residual learning and batch normalization. Subsequently, the blocks are aggregated, and the image is reconstructed, akin to the 3D block-matching algorithm.

Researchers in [15] proposed the attention-directed CNN (ADNet) for image denoising, consisting of four blocks scattering (SB), feature enhancement (FEB), attention (AB), and reconstruction (RB) totaling 17 layers. SB, with 12 layers of Dilated Conv + BN + ReLU and Conv + BN + ReLU, enhances the effectiveness, performance, and depth reduction of the denoising framework. FEB incorporates three types of layers (Conv + BN + ReLU, Conv, and Tanh), and AB is a single convolution layer. [29] introduced the Noise Estimation Removal Network (NERNet) for noise reduction, consisting of modules for noise estimation and noise cancellation. The architecture integrates symmetric dilated blocks and pyramid feature fusion, adjusting to the noise level map for effective noise reduction. Gai and Bao in [30] utilized an upgraded CNN, MP-DCNN, for adaptive residual denoising. The model uses Leaky ReLU for noise extraction, employs SegNet for edge information retrieval, and utilizes MSE and perceptual loss for image reconstruction. Zhang et al. [31] proposed a dictionary learning model for mixtures of Gaussian distribution (MOG), adopting a minimization problem with sparse coding, dictionary updating, and hierarchical mapping functions to address the vanishing problem. Also, they proposed SANet which employed band aggregation, deep mapping, and convolutional separation blocks for noise removal. The architecture divides input noise into smaller blocks, maps and conceals each band, and aggregates all maps to create the output. Li et al. [32] suggested a detail-preserving CNN (DRCNN) that focuses on integrating high-frequency image material. DRCNN includes Generalization Module (GM) and Detail Preserving Module (DRM), lacking batch normalization, and addresses a detail loss function minimization problem. Xu et al. [33] introduced Bayesian deep matrix factorization (BDMF) for multiple image denoising, utilizing deep neural networks (DNN) for low-rank components and optimization through stochastic gradient variation Bayes. Jin et al. [34] proposed a classifier/regression CNN for image denoising, with a classifier network detecting impulse noise and a regression network restoring noisy pixels based on the classifier's prediction. Fang and Zeng [24] suggested the CNN variation model (CNN-VM) for picture denoising, employing EdgeNet with multiple scale residual blocks (MSRB) and edge regularization for feature extraction. Total variation regularization enhances shape edge performance, and Bregman splitting technique is used for solution discovery.

There are also innovative methods were also employed for network architecture, with residual learning being noteworthy as it focused on isolating noise rather than noise-free images. However, a fundamental issue persisted training these models required specificity to noise types and levels. Any change in the target noise necessitated a complete retraining from scratch. Deep neural networks have gained remarkable attention due to their exceptional performance in image-related tasks. Yet, the extended training duration, the challenge of hyperparameter selection, and other complexities inherent to DL cannot be overlooked. Ongoing efforts, such as batch normalization, aim to address these issues. Another drawback of DL methods is their limited performance when dealing with untrained noise types. For example, while BM3D can mitigate noise in images with mixed noise types, DL networks trained on specific noise types like Gaussian noise struggle with such scenarios. This limitation can be partly alleviated by training deep networks on more diverse real-world data [13].

III. Material and Methods

In this section, the different dataset groups used in the study are described, the proposed methodology is explained, and the evaluation metrics are presented.

A. Datasets

The proposed denoising system employs two medical datasets for training and testing, carefully selected to align with the objectives of this study. The first dataset utilized for evaluation is the chest X-ray (CXR) dataset [35], which comprises a variety of images representing different categories such as COVID-19, SARS, ARDS, and Streptococcus. Fig. 3 represent samples form the first dataset.

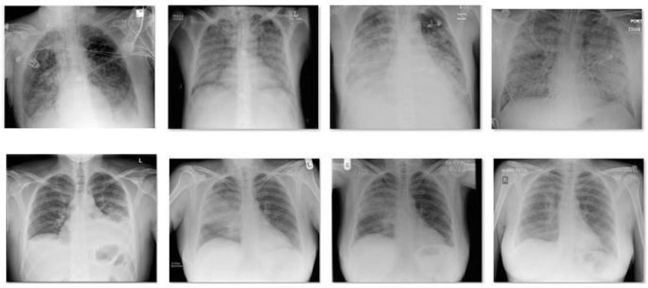

Fig. 3. Samples from the first dataset

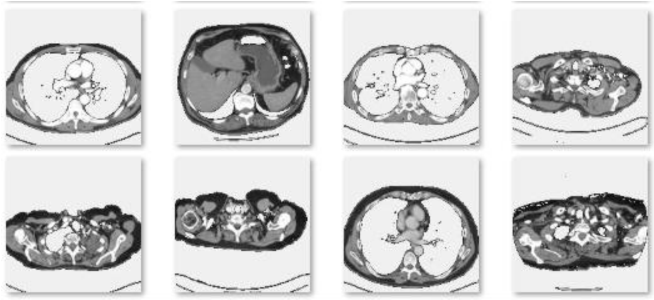

Fig. 4. Samples from the second dataset

In the second set of experiments, we utilize the CT Medical Images dataset [36], a subset of archived images from cancer imaging. These images are extracted from the central portion of computed tomography (CT) images and encompass a total of 475 images sourced from 69 distinct patients. This dataset was curated to assess various techniques for investigating trends in CT image data, specifically in relation to contrast utilization and patient age. Fig. 4 represent samples from this dataset.

B. *Proposed Method*

The process involves four key stages. Initially, images are categorized into training and testing sets, where training data is used to train the model, and test data assesses its performance. The model undergoes training through an automatic coding method and the training dataset. Next, the data is fed into a CNN for additional learning. Finally, the testing data evaluates the system's performance. The system comprises four main blocks: the original image, noisy image generation, denoising via an autoencoder, and denoising using a CNN, each playing a vital role in the noise reduction process. we have detailed the steps of the proposed method in Fig. 5.

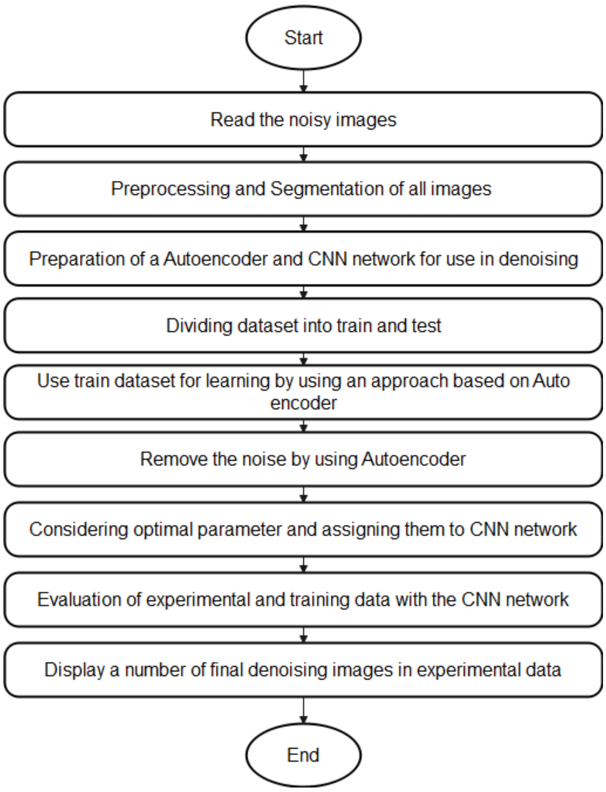

Fig. 5. The proposed method

This first step involves the selection of the database for processing and applying denoising using the CNN. In the second stage of this process, a crucial step unfolds as all the images undergo comprehensive preprocessing to ensure they are suitably prepared for subsequent analysis and processing. This meticulous preparation sets the foundation for effective data manipulation. Following this, in the third step, the groundwork is laid for the utilization of an autoencoder network, which plays a pivotal role in the denoising of images. This network, a cornerstone of the denoising process, is prepared with great care and precision. Autoencoder aims to reduce dimensionality and discover features in the data. Constraints on hidden units prevent the model from learning identity mappings, and it's trained to predict its input. The basic structure, illustrated in Fig. 6, includes input (x), encoding (y) via an encoder (f), and reconstruction (r).

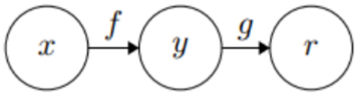

Fig. 6. General view of an auto-encryptor

The denoising autoencoder is designed to resist noise better by capturing high-level features and remaining robust to small input variations. It takes noisy input data and aims to produce clean, noise-free data. In our study, we introduce input noise by varying sample values before training and use CNNs. The process involves two steps: first, the model learns from the dataset using an autoencoder-based approach, and then noise is removed using another autoencoder. The output of this step is fed into a CNN to enhance image quality. The description and parameters of CNN layers and Auto Encoders are describing in Table I.

TABLE I. DESCRIPTION OF CNN LAYERS AND AUTO ENCODER PARAMERERS

Part	Parameter	Value
Images	Images size	120×120×3
CNN	layers CNN	imageInputLayer convolution2dLayer batchNormalization leakyReluLayer fullyConnectedLayer softmaxLayer classificationLayer
	Max Epochs	300
	ValidationFrequency	30
	Batch size	16
Auto Encoder	Number of Hidden Neurons	500
	Activation Function	Sig
	Ratio of noising features	0.4

According to Table I, the description outlines the parameters for a CNN and an Auto Encoder. The image-related parameters for the CNN include an image size of 120×120×3 pixels. The CNN architecture involves layers such as imageInputLayer, convolution2dLayer, batchNormalization, leakyReluLayer, fullyConnectedLayer, softmaxLayer, and classificationLayer. Training parameters for the CNN include a maximum of 300 epochs, validation frequency set to every 30 epochs, and a batch size of 16. The Auto Encoder specifications include 500 hidden neurons, a sigmoid activation function, and a 0.4 ratio for noising features.

Moving along to the fourth step, a pivotal division takes place within the dataset itself. The dataset is thoughtfully categorized into two subsets: the training dataset and the test dataset. This categorization is essential for systematically training and evaluating the performance of the proposed system. In the fifth step, an ingenious approach grounded in autoencoder principles is employed. This approach facilitates learning from the dataset, an integral part of the denoising process. The knowledge gleaned from this step forms the basis for subsequent noise removal. Subsequently, in the sixth step, the expertise acquired through the autoencoder-based approach is harnessed to effectively remove noise from the images. This marks a critical advancement in enhancing the visual quality of the images. The seventh step ushers in the utilization of the denoised output as input for a CNN, further advancing the image processing and denoising journey. Continuing to the eighth step, the parameters and weightings of the network's layers are meticulously fine-tuned and applied to the CNN. This step marks the calibration of the CNN for optimal performance. Subsequent to this calibration, in the ninth step, the system is subjected to rigorous testing using data from the designated testing section. Here, the system's performance is subjected to a thorough evaluation, and its capability as a tester for the proposed system is assessed. In the tenth step, the evaluation process extends to encompass the experimental and simulation data, which are rigorously scrutinized using the optimized CNN network. Finally, in the last step, the culmination of this meticulous process is celebrated as a selection of the final denoised images is presented. These images represent the successful outcome of the entire experimental endeavor, reflecting the power, and efficacy of the applied denoising techniques.

C. Evaluation Metrics

One of the key benchmarks employed to assess the effectiveness of noise reduction techniques is the utilization of root mean square error (RMSE) deviation, as defined in (1). This criterion, as computed through the provided equations, quantifies the extent of disparity between the original image and the noise-reduced image. It's evident that a lower value for this parameter signifies a superior outcome.

$$RMSE = \sqrt{\frac{\sum_{i=1}^{N}(x_{ij} - y_{ij})^2}{N}} \tag{1}$$

where N represents the total number of image pixels, with x_{ij} denoting the pixel value in the original image at position i and j, and y_{ij} indicating the pixel value in the denoised image at the same position.

Signal-to-noise ratio (SNR) stands out as a vital evaluation metric in noise removal studies. This research leverages SNR to gauge both the distortion levels within the denoised image relative to the original and the overall image quality. Essentially, this metric quantifies changes in pixel intensity between the original and noise-reduced images. A higher SNR value signifies reduced distortion in comparison to the original image, indicating superior image quality. Peak signal-to-noise ratio (PSNR), as determined by (2), serves as a key component in this evaluation.

$$PSNR = 10 \times log_{10} \frac{255^2}{MSE} \tag{2}$$

IV. Results

The testing system boasts significant specifications. It runs on an 11th Gen Intel® Core™ i3-1115G4 processor, clocked at 3.00GHz. with 8.0 GB of RAM and a 260 GB SSD, it offers efficient memory and storage capabilities. Operating on Microsoft Windows 10 Ultimate, it provides a stable software environment. Additionally, MATLAB R2022a serves as the primary programming language, enabling versatile computational tasks. These specifications collectively establish the system's suitability for conducting research experiments and analyses.

We present the outcomes of our evaluations. To achieve this, we provide a comprehensive analysis of the evaluation results for each of the datasets introduced in the preceding section. Moreover, we will delve into the evaluation criteria, dissecting their impact on the results. It's important to note that we have considered the significance of training data volume for methods utilizing learning algorithms. As a result, we have incorporated the size of the training dataset as an evaluation parameter. Indeed, the results presented in this section encompass various training dataset sizes, specifically, 50% (with a corresponding testing size of 50%) and 70% (with a corresponding testing size of 30%). Our intent in varying the training dataset size is to discern the extent of influence on the compared methods as the training data volume fluctuates. Subsequently, we will proceed to delineate the evaluation results for each dataset, shedding light on the nuances uncovered during our analysis.

A. Results of the CXR Dataset

The initial set of findings within this section pertains to the assessment of PSNR and RMSE metrics on the CXR dataset. As a result, the results from the evaluation of both the proposed method and the base method based on these criteria are visually depicted in Fig. 7 and Fig. 8.

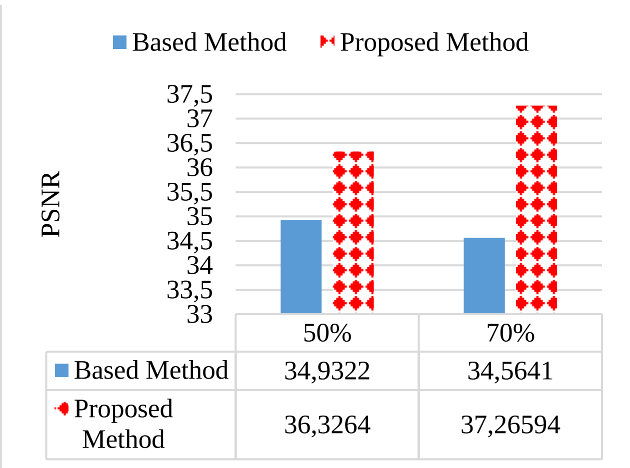

Fig. 7. PSNR benchmark evaluation results on CXR dataset

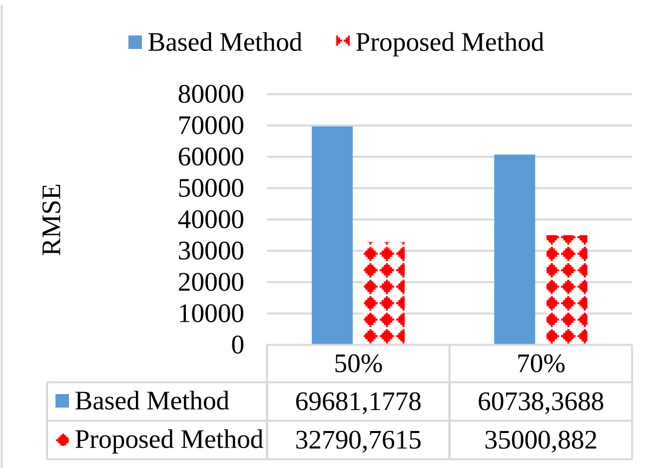

Fig. 8. The evaluation results of the RMSE criterion on the CXR dataset

As depicted in Fig. 7 and Fig. 8, it becomes evident that the proposed approach outperforms the base method consistently. In essence, when evaluating the CXR dataset, the proposed method excels across both evaluation criteria and various training dataset sizes, yielding significantly superior results in comparison to the base method. A closer examination of the results laid out in this section unmistakably highlights the favorable performance of the proposed method. This is manifested in the notably lower error rates exhibited by the proposed method in contrast to the base method. Consequently, the images generated through the proposed method are of markedly superior quality. These findings underscore the robustness and effectiveness of the proposed approach, reinforcing its suitability for noise reduction tasks and its capacity to consistently deliver higher-quality results, particularly when confronted with varying training dataset sizes.

B. *Results of CT Medical Images Dataset*

In this section, similar to the preceding one, we will delve into the evaluation outcomes for each of the compared methods using the CT Medical Images dataset. These experiments encompass the inclusion of variations in the size of the training dataset as a dynamic parameter for the study. Within the ensuing Fig. 9 and Fig. 10, we present the evaluation results for each of the compared methods within this dataset.

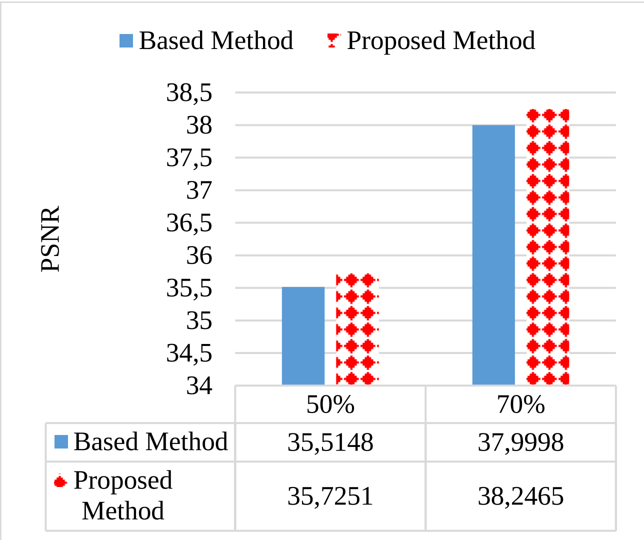

Fig. 9. PSNR benchmark evaluation results on CT medical images dataset

The results depicted in the aforementioned Fig. 9 and Fig. 10 substantiate that the proposed method outperforms the compared method when considering the PSNR criterion. Notably, variations in the size of the training dataset have failed to diminish the superiority exhibited by the proposed method. In fact, it is evident that the proposed method consistently outshines the compared method, even when the training dataset size is altered, as observed in the PSNR criterion.

However, a closer examination of the results presented in Fig. 10 reveals a divergence in performance between the two methods, with the compared method outperforming our approach in this specific criterion. This divergence is elucidated by the RMSE criterion, which indicates that the compared method yields lower error rates than the proposed method. A comprehensive summary of these evaluation results, underscoring the supremacy of the proposed method, is encapsulated in Table II. The ratios given in Table II are obtained by calculating the percentage of the difference between the proposed method and the base method to the base method.

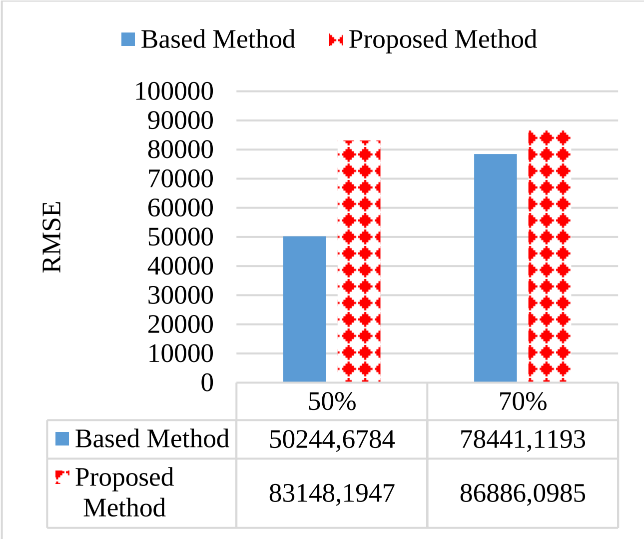

Fig. 10. RMSE evaluation results on the CT medical images dataset

TABLE II. THE IMPROVEMENT RATE OF THE PROPOSED METHOD COMPARED TO THE BASE METHOD

Dataset	Parameter	Comparison rates	
		50% - 50% Data Division	70% - 30% Data Division
CXR	PSNR	3.99%	7.82%
	RMSE	52.94%	42.37%
CT Medical Images	PSNR	0.59%	0.65%
	RMSE	-65.49%	-10.77%

Table II presents the comparison between the proposed method and the base method. In this comparison, a positive improvement, i.e. increase, is expected for PSNR and a negative improvement, i.e. decrease, is expected for RMSE. As can be seen in Table II, for the CXR data, both metrics are improved for both 50-50% data split and 70-30% data split. For CT medical images, although there is a slight improvement in the PSNR metric, there is no improvement in the RMSE metric, on the contrary, the proposed method gives worse results. According to these results, it can be stated that the auto encoder method fails for CT medical image but succeeds for CXR dataset.

In the case of the CT Medical Images dataset, the proposed method still achieves a commendable 5% improvement in PSNR, demonstrating its effectiveness in enhancing image quality. However, it's noteworthy that the RMSE criterion shows a negative improvement rate of -65%. While this may initially appear counterintuitive, it suggests that the proposed method, in certain scenarios, may yield slightly higher errors compared to state-of-the-art methods. Nonetheless, the combined results presented in Table 1 affirm the overall superiority of the proposed method in noise removal tasks across these datasets.

V. DISCUSSION

The results outlined in Table 1 not only highlight the significant effectiveness of the proposed noise removal method but also reveal its superiority over state-of-the-art approaches. The results substantial advancement underscores the method's prowess in achieving superior noise reduction quality. The consistent outperformance of the proposed method, especially when applied to the CXR dataset, signifies its robustness and reliability. Notably, this superiority remains resilient even when considering variations in the size of the training dataset, establishing it as a defining characteristic of the proposed method. This hallmark performance is indicative of the method's ability to adapt and maintain effectiveness across different data configurations.

The innovative dual-step approach to noise removal, integrating an autoencoder-based method for knowledge acquisition and subsequently employing autoencoder techniques in conjunction with a CNN, emerges as a pivotal factor in the success of the proposed method. This multi-step process plays a critical role in maximizing the quality of the resulting images, ensuring not only the removal of noise but also the preservation of essential image features. By strategically combining these techniques, the proposed method excels in noise reduction tasks, demonstrating a nuanced and sophisticated approach to addressing the challenges associated with medical image denoising.

It is crucial to emphasize the broader implications of the proposed method in the context of medical imaging. The superior performance observed on the CXR dataset suggests that the method holds significant promise for applications such as respiratory and cardiac imaging, where image quality is paramount for accurate diagnosis and treatment planning. Moreover, the consistent outperformance across datasets underscores the method's versatility, making it a robust candidate for a wide range of medical imaging modalities.

The findings of this study contribute not only to the advancement of medical image denoising but also provide valuable insights for future research directions. The success of the dual-step approach opens avenues for exploring similar strategies in other image processing tasks, fostering innovation in the broader field of computer vision. Additionally, the discussion prompts consideration of potential refinements or extensions to the proposed method, such as exploring variations in the architecture or incorporating additional layers to further enhance its adaptability and generalization capabilities.

VI. CONCLUSION

DL studies have been successfully applied in many different fields, especially in the last decade. Image processing is one of the most common among these fields. One of the most important limitations for DL and image processing studies applied in many different fields such as health [37], [38], education [39], [40], communication [41], industry, agriculture [42] etc. is the noise in the data. Noise in medical images arises from various sources, including transmission and environmental factors, resulting in types like Gaussian, Poisson, blur, speckle, and salt-and-pepper noise. Noise reduction is vital in medical imaging, with filters like median, Gaussian, and Wiener customized for specific noise types. However, no universal solution meets all medical image denoising needs.

This study presents a tailored medical image noise reduction method, Automatic Noise Removal via Convolutional Neural Networks, using a two-step algorithm. It categorizes images into training and testing sets and employs automatic coding on the training data, training a CNN. Testing data evaluates the system. Efficacy was assessed using MATLAB, and a basic CNN method was implemented. Evaluation results, based on RMSE and PSNR criteria on datasets, clearly affirm the proposed method's consistent superiority over the base method.

This research highlights the effectiveness of CNN architectures in noise removal from images. The second chapter offers an overview of various CNN-based image denoising techniques, acknowledging both strengths and limitations. Challenges include limited memory capacity for CNN programs and the complexity of unsupervised denoising tasks. Furthermore, CNN methods remain relatively underutilized in medical image denoising. Future research may explore memory allocation for CNN tasks and the integration of these methods into expanding computer systems for disease diagnosis. Additionally, researchers in this field could draw inspiration from the approach presented in this study to devise novel image denoising methods, potentially by combining it with existing techniques for enhanced noise reduction.

REFERENCES

[1] A. A. Saraiva, M. S. de Oliveira, P. B. de Moura Oliveira, E. J. Solteiro Pires, N. M. Fonseca Ferreira, and A. Valente, “Genetic algorithm applied to remove noise in DICOM images,” J. Inf. Optim. Sci., vol. 40, no. 7, pp. 1543–1558, 2019, doi: 10.1080/02522667.2019.1597999.

[2] S. Rani, Y. Chabrra, and K. Malik, “An Improved Denoising Algorithm for Removing Noise in Color Images,” Eng. Technol. Appl. Sci. Res., vol. 12, no. 3, pp. 8738–8744, 2022, doi: 10.48084/etasr.4952.

[3] D. G. Kim, M. Hussain, M. Adnan, M. A. Farooq, Z. H. Shamsi, and A. Mushtaq, “Mixed Noise Removal Using Adaptive Median Based Non-Local Rank Minimization,” IEEE Access, vol. 9, pp. 6438–6452, 2021, doi: 10.1109/ACCESS.2020.3048181.

[4] A. Mukherjee, S. Sarkar, and S. K. Saha, “Segmentation of natural images based on super pixel and graph merging,” IET Comput. Vis., vol. 15, no. 1, pp. 1–11, 2021, doi: 10.1049/cvi2.12008.

[5] A. Jindal, N. Aggarwal, and S. Gupta, “An Obstacle Detection Method for Visually Impaired Persons by Ground Plane Removal Using Speeded-Up Robust Features and Gray Level Co-Occurrence Matrix,” Pattern Recognit. Image Anal., vol. 28, no. 2, pp. 288–300, 2018, doi: 10.1134/S1054661818020086.

[6] R. Chauhan, K. K. Ghanshala, and R. C. Joshi, “Convolutional Neural Network (CNN) for Image Detection and Recognition,” ICSCCC 2018 - 1st Int. Conf. Secur. Cyber Comput. Commun., pp. 278–282, 2018, doi: 10.1109/ICSCCC.2018.8703316.

[7] Y. Zhang, “A Better Autoencoder for Image: Convolutional Autoencoder,” pp. 1–7, 2015.

[8] A. Semwal, A. Chamoli, and A. Semwal, “A SURVEY : On Image Denoising And Its Various Techniques,” Int. Res. J. Eng. Technol., pp. 1565–1568, 2017.

[9] K. Zhang, W. Zuo, and L. Zhang, “FFDNet: Toward a fast and flexible solution for CNN-Based image denoising,” IEEE Trans. Image Process., vol. 27, no. 9, pp. 4608–4622, 2018, doi: 10.1109/TIP.2018.2839891.

[10] A. E. Ilesanmi and T. O. Ilesanmi, “Methods for image denoising using convolutional neural network: a review,” Complex Intell. Syst., vol. 7, no. 5, pp. 2179–2198, 2021, doi: 10.1007/s40747-021-00428-4.

[11] B. Goyal, A. Dogra, S. Agrawal, B. S. Sohi, and A. Sharma, "Image denoising review: From classical to state-of-the-art approaches," Inf. Fusion, vol. 55, pp. 220–244, 2020, doi: 10.1016/j.inffus.2019.09.003.

[12] S. Sudha, G. R. Suresh, and R. Sukanesh, "Speckle Noise Reduction in Satellite Images Using Spatially Adaptive Wavelet Thresholding," Int. J. Comput. Sci. Inf. Technol., vol. 3, no. 2, pp. 3432–3435, 2012.

[13] A. A. A. Goshtasby, "Advances in Computer Vision and Pattern Recognition," Image Regist. Princ. Tools methods, pp. 7–66, 2012, [Online]. Available: http://www.springerlink.com/index/10.1007/978-1-4471-2458-0

[14] K. Bajaj, D. K. Singh, and M. A. Ansari, "Autoencoders Based Deep Learner for Image Denoising," Procedia Comput. Sci., vol. 171, pp. 1535–1541, 2020, doi: 10.1016/j.procs.2020.04.164.

[15] P. Svoboda, M. Hradis, D. Barina, and P. Zemcik, "Compression artifacts removal using convolutional neural networks," J. WSCG, vol. 24, no. 2, pp. 63–72, 2016.

[16] P. Vincent, H. Larochelle, Y. Bengio, and P. A. Manzagol, "Extracting and composing robust features with denoising autoencoders," Proc. 25th Int. Conf. Mach. Learn., pp. 1096–1103, 2008, doi: 10.1145/1390156.1390294.

[17] F. Agostinelli, M. R. Anderson, and H. Lee, "Adaptive multi-column deep neural networks with application to robust image denoising," Adv. Neural Inf. Process. Syst., 2013.

[18] L. Gondara, "Medical Image Denoising Using Convolutional Denoising Autoencoders," IEEE Int. Conf. Data Min. Work. ICDMW, vol. 0, pp. 241–246, 2016, doi: 10.1109/ICDMW.2016.0041.

[19] B. Du et al., "Stacked Convolutional Denoising Auto-Encoders for Feature Representation," IEEE Trans. Cybern., vol. 47, no. 4, pp. 1017–1027, 2017.

[20] S. S. Roy, S. I. Hossain, M. A. H. Akhand, and K. Murase, "A robust system for noisy image classification combining denoising autoencoder and convolutional neural network," Int. J. Adv. Comput. Sci. Appl., vol. 9, no. 1, pp. 224–235, 2018, doi: 10.14569/IJACSA.2018.090131.

[21] J. Lehtinen et al., "Noise2Noise: Learning image restoration without clean data," 35th Int. Conf. Mach. Learn. ICML 2018, vol. 7, pp. 4620–4631, 2018.

[22] A. Krull, T. O. Buchholz, and F. Jug, "Noise2void-Learning denoising from single noisy images," Proc. IEEE Comput. Soc. Conf. Comput. Vis. Pattern Recognit., vol. 2019-June, pp. 2124–2132, 2019, doi: 10.1109/CVPR.2019.00223.

[23] J. Batson and L. Royer, "Noise2Seif: Blind denoising by self-supervision," 36th Int. Conf. Mach. Learn. ICML 2019, vol. 2019-June, pp. 826–835, 2019.

[24] Y. Fang and T. Zeng, "Learning deep edge prior for image denoising," Comput. Vis. Image Underst., vol. 200, 2020, doi: 10.1016/j.cviu.2020.103044.

[25] X. Fu, S. Jia, L. Zhuang, M. Xu, J. Zhou, and Q. Li, "Hyperspectral Anomaly Detection via Deep Plug-and-Play Denoising CNN Regularization," IEEE Trans. Geosci. Remote Sens., vol. 59, no. 11, pp. 9553–9568, 2021, doi: 10.1109/TGRS.2021.3049224.

[26] T. Wu, W. Li, S. Jia, Y. Dong, and T. Zeng, "Deep multi-level wavelet-CNN denoiser prior for restoring blurred image with cauchy noise," IEEE Signal Process. Lett., vol. 27, pp. 1635–1639, 2020, doi: 10.1109/LSP.2020.3023299.

[27] B. Ahn and N. I. Cho, "Block-Matching Convolutional Neural Network for Image Denoising," 2017, [Online]. Available: http://arxiv.org/abs/1704.00524

[28] K. Zhang, W. Zuo, Y. Chen, D. Meng, and L. Zhang, "Beyond a Gaussian denoiser: Residual learning of deep CNN for image denoising," IEEE Trans. Image Process., vol. 26, no. 7, pp. 3142–3155, 2017, doi: 10.1109/TIP.2017.2662206.

[29] B. Guo, K. Song, H. Dong, Y. Yan, Z. Tu, and L. Zhu, "NERNet: Noise estimation and removal network for image denoising," J. Vis. Commun. Image Represent., vol. 71, 2020, doi: 10.1016/j.jvcir.2020.102851.

[30] S. Gai and Z. Bao, "New image denoising algorithm via improved deep convolutional neural network with perceptive loss," Expert Syst. Appl., vol. 138, 2019, doi: 10.1016/j.eswa.2019.07.032.

[31] L. Zhang, Y. Li, P. Wang, W. Wei, S. Xu, and Y. Zhang, "A separation–aggregation network for image denoising," Appl. Soft Comput. J., vol. 83, 2019, doi: 10.1016/j.asoc.2019.105603.

[32] X. Li et al., "Detail retaining convolutional neural network for image denoising," J. Vis. Commun. Image Represent., vol. 71, 2020, doi: 10.1016/j.jvcir.2020.102774.

[33] D. Yin et al., "Speckle noise reduction in coherent imaging based on deep learning without clean data," Opt. Lasers Eng., vol. 133, 2020, doi: 10.1016/j.optlaseng.2020.106151.

[34] L. Jin, W. Zhang, G. Ma, and E. Song, "Learning deep CNNs for impulse noise removal in images," J. Vis. Commun. Image Represent., vol. 62, pp. 193–205, 2019, doi: 10.1016/j.jvcir.2019.05.005.

[35] "https://www.kaggle.com/datasets/tawsifurrahman/covid19-radiography-database."

[36] "https://www.kaggle.com/datasets/kmader/siim-medical-images".

[37] R. Butuner, & M. H. Calp. Diagnosis and Detection of COVID-19 from Lung Tomography Images Using Deep Learning and Machine Learning Methods. International Journal of Intelligent Systems and Applications in Engineering, 10(2), 190-200, 2022.

[38] B. Guler Ayyildiz, R. Karakis, B. Terzioglu, & D. Ozdemir. Comparison of deep learning methods for the radiographic detection of patients with different periodontitis stages. Dentomaxillofacial Radiology, 53(1), 32-42, 2024.

[39] Q. Gazawy, S. Buyrukoglu and A. Akbas, "Deep Learning for Enhanced Education Quality: Assessing Student Engagement and Emotional States," 2023 Innovations in Intelligent Systems and Applications Conference (ASYU), Sivas, Türkiye, 2023, pp. 1-8, doi: 10.1109/ASYU58738.2023.10296748.

[40] O. Güler, & İ. Yücedağ, Artırılmış Gerçeklik: Montaj ve Bakım Uygulamalarında El Tanıma Teknolojisi İle Etkileşim Çalışmaları. Paper presented at the 20. Akademik Bilişim Konferansı, Karabük. 2018. http://indexive.com/uploads/papers/pap_indexive15949797202147483647.pdf

[41] N. Daldal, Z. A. Sezer, M. Nour, A. Alhudhaif, K. Polat, A New Generation Communication System Based on Deep Learning Methods for the Process of Modulation and Demodulation from the Modulated Images, Mathematical Problems in Engineering, vol. 2022, Article ID 9555598, 13 pages, 2022. https://doi.org/10.1155/2022/9555598.

[42] R. Bütüner and M. H. Calp, (2023). Robotic Systems and Artificial Intelligence Applications in Agriculture. Current Studies in Technology, Innovation and Entrepreneurship, 145.